PERGAMON

International Journal of Heat and Mass Transfer 46 (2003) 113–125

International Journal of HEAT and MASS TRANSFER

www.elsevier.com/locate/ijhmt

Heat transfer of a row of three butane/air flame jets impinging on a flat plate

L.L. Dong, C.W. Leung *, C.S. Cheung

Department of Mechanical Engineering, The Hong Kong Polytechnic University, Hung Hom, Kowloon, Hong Kong

Received 29 January 2002; received in revised form 7 June 2002

Abstract

Experiments were performed to investigate the heat transfer characteristics of a row of three premixed, laminar, butane/air flame jets impinging on a water-cooled flat plate. The between-jet interference was found to reduce the heat transfer rate in the jet-to-jet interacting zone due to the depressed combustion. The interference became stronger when the jet-to-jet spacing and/or the nozzle-to-plate distance were/was small. The positive pressure existed in the between-jet interacting zone caused the asymmetric flame and heat transfer distribution of the side jet. The meeting point of the spreading wall jets of the central and the side jets did not occur at the midpoint of the neighboring jets, but at a location shifted slightly outwards. The maximum local heat flux and the maximum area-averaged heat flux occurred at a moderate nozzle-to-plate distance of 5d with a moderate jet-to-jet spacing of 5d. The lowest area-averaged heat flux was produced when both the jet-to-jet spacing and the nozzle-to-plate distance were small. Comparing with a single jet under the same experimental conditions, the heat transfer rates in both the stagnation point and the maximum heat transfer point were shown to be enhanced in a row of three-jet-impingement system. The present study provided detailed information on the heat transfer characteristics of a row of three in-line impinging flame jets, which had rarely been reported in previous study.

Keywords: Butane/air combustion; Impingement heat transfer; Laminar; Multiple flame jets

1. Introduction

Impinging isothermal and flame jets have been widely used in heating, cooling and drying processes for their enhanced convective heat transfer rates. Multiple jets are needed to employ when a large surface area is required to be heated or cooled [1]. Use of multiple jets can also enhance heating/cooling uniformity by creating several impingement zones. From the viewpoint of the design of equipment using multiple jets, detailed and accurate data are required, which cannot be predicted from those of the single jet. This is because the influence of the jet-to-jet interaction cannot be inferred from single jet data [2].

Multiple impinging isothermal air jets have been investigated quite extensively. Fluid mechanics and heat transfer characteristics of impingement systems with different jet number and jet arrangement pattern have been studied. The simplest system consists of a pair of jets. The relevant information on the flow field, pressure distribution and heat transfer in this twin-jet system can be referred to the previous work [3–9]. In practical application, a row or multiple rows of impinging jets are often used. In multiple rows of impinging jets, both in-line and staggered arrangements of the jets can be employed. Relevant investigations can be found elsewhere [10–18].

A row of air jets have also been studied by many investigators [19–22]. Saad et al. [22] investigated jet array system consisting of three identical confined slot jets with symmetrical exhaust ports in the confinement surface. It was found that the critical S/H ratio, at which the non-interacting multiple impinging slot jets were

* Corresponding author. Tel.: +852-2766-6651; fax: +852-2365-4703.

E-mail address: mmcwl@polyu.edu.hk (C.W. Leung).

0017-9310/03/$ - see front matter
PII: S0017-9310(02)00225-9

Nomenclature

A	integration area (m^2)
B	nozzle width (m)
d	nozzle exit diameter (m)
h_{chem}	enthalpy due to chemical reaction (J/kg)
$h_{chem,H}$	enthalpy due to the recombination of hydrogen atoms (J/kg)
h_{eq}	total enthalpy ($= h_f + h_{chem}$) (J/kg)
h_f	sensible enthalpy (J/kg)
H	distance between the nozzle and the impingement plate (m)
Le_H	Lewis number based upon the diffusion of hydrogen atoms in the flame gas
Nu	Nusselt number ($= \alpha d/\lambda$)
$\dot{q}$	local heat flux density (W/m^2)
$\bar{q}$	area-averaged heat flux density (W/m^2)
r	radial distance from midpoint of the two nozzles (m)
Re	Reynolds number ($= u_{out}d/\nu$)
R_0	air supply pipe inside radius (m)
S	distance between the centers of the two nozzles (m)
u	velocity of butane/air mixture (m/s)
x	the streamwise axis (m)
y	the spanwise axis (m)

Greek symbols

α	heat transfer coefficient ($W/m^2\,K$)
β	the velocity gradient near the stagnation point ($= (dv/dr)_{r\to 0}$)
λ	thermal conductivity (W/mK)
ν	kinematic viscosity (m^2/s)
ϕ	equivalence ratio (=(stoichiometric air/fuel volume ration)/actual air/fuel volume ratio))

Superscript

–	averaged value

Subscripts

b	stagnation body or target
e	edge of boundary layer
f	flame jet
out	at the nozzle exit surface

separated from the interaction ones, was between 1 and 0.75. Goldstein and Timmers [23] investigated a row of three impinging air jets. They found that at low H/d ratio of 2, the high crossflow caused the non-circular shape of the constant Nusselt curves around the outer jets and outward movement of the maximum Nu of the outer jets. Goldstein and Seol [24] investigated a row of impinging air jets, and found that the jets with the closer jet-to-jet spacing were able to produce larger average Nusselt number. A single row of jets appears to be more efficient than a slot jet for maximizing the heat mass transfer with the same mass flow rate. Koopman and Sparrow [25] investigated a row of impinging air jets and found that a local maximum heat transfer coefficient occurred at the midway between adjacent jets, due to the collision of the spreading flows from two impinged adjacent jets. This maximum heat transfer coefficient becomes prominent at smaller H/d ratio, larger Reynolds number, and when the jets are more closely spaced. The highest spanwise-averaged coefficients are at the impingement line, except at closest separation where they occur along the line of $x/d = 0.5$. Gardon and Akfirat [13] investigated a system of three impinging unconfined slot jets. They found that the pressure and heat flux distributions in the impingement region of the middle jet was substantially the same as those of a single unconfined impinging jet. Marked secondary peaks in the heat transfer rate at the points midway between adjacent nozzles were found for the relatively small nozzle-to-plate spacing of $H/B = 4$, but they were not occurred for a large spacing of $H/B = 16$. It has been verified that in multiple jet systems, the spent flow from upstream jets (i.e., the crossflow) deteriorates the thermal performance of the downstream jets [26]. Gundappa et al. [27] studied a row of three jets and found that this crossflow problem could be eliminated when jet tubes were used to replace the orifice plates. Al-Sanea [28] quantified the reduction of Nusselt number to be as much as 60% due to the presence of crossflow. Seyedein et al. [29] carried out a numerical investigation to reduce non-uniformity of heat transfer caused by crossflow. They found that inclining the confinement surface could accelerate the exhaust flow, which could lead to a more uniform Nusselt number distribution.

Comparing to the numerous studies relating to multiple impinging air jets, much fewer investigations have been performed on multiple impinging flame jets. The studies of flame jet have mainly focused on the single jet [30–37]. Malikov et al. [37] studied the heat transfer in a rapid heating furnace with a multi-jet combustion chamber both experimentally and numerically. Mohr et al. [38] investigated the between-jet interference of a pair of impinging radial flame jets. Wu et al. [39] investigated a row of three radial flame jets. High pressure was observed in the interaction region between the two neighboring nozzles, with the highest value occurred at the midpoint between them. Effect of jet-to-jet spacing on heat transfer was examined. It was observed that

high surface heat fluxes were obtained at a moderate jet-to-jet spacing of $S/R_0 = 8$. It is due to the co-existence of the higher temperature difference between the gas/flame and the impingement plate, and the stronger impact resulted from the higher pressure in the interaction zone. However, studies on multiple impinging in-line flame jets have been rarely reported so far, in spite of their wide usage in application such as domestic gas appliances. Viskanta [40,41] has reviewed the studies on impinging jets and recommended the study on multiple impinging flame jets should be carried out.

A row of three in-line flame jets had been chosen in the present study. Three jets were selected because it could represent a large array of impinging jet system. A center jet surrounded by two side jets, which will experience interference from the two neighboring jets, provides the characteristics of each jet in a large array except the end jets. Butane gas has been selected in the present study. Experiments were carried out to study the influences of non-dimensional nozzle-to-plate distance (i.e., H/d) and jet-to-jet spacing (i.e., S/d) on the flame structures and the heat transfer characteristics of both the center and the side jets. The S/d ratio was varied from 2.6 to 7 to cover small, moderate and large jet-to-jet spacing. The H/d ratio was selected from 2 to 8 to include the length of the flame's inner cone. Reynolds number was chosen to be 900 to produce laminar flames. All the tests were performed at the stoichiometric condition.

2. Experimental setup and method

The impinging flame jet system of the present study consisted two parts: the heat generation system and the heat absorption system, as shown schematically in Fig. 1.

There were two kinds of flame holder. The first kind consisted of three identical 50 mm long brass tubes with 5 mm inner diameter. The other consisted of a single brass tube with the same length and diameter. The butane gas and compressed air were metered and premixed in a brass cylinder, before entering the cylindrical aluminum equalization chamber via a 200 mm long stainless steel tube. The equalization chamber was filled with stainless steel beads to make the flow more uniform and to prevent the flame from flashing back. The mixture then entered the flame holder, and the flame was ignited and stabilized at the rim. The inside surface of the flame holder was polished to facilitate a more

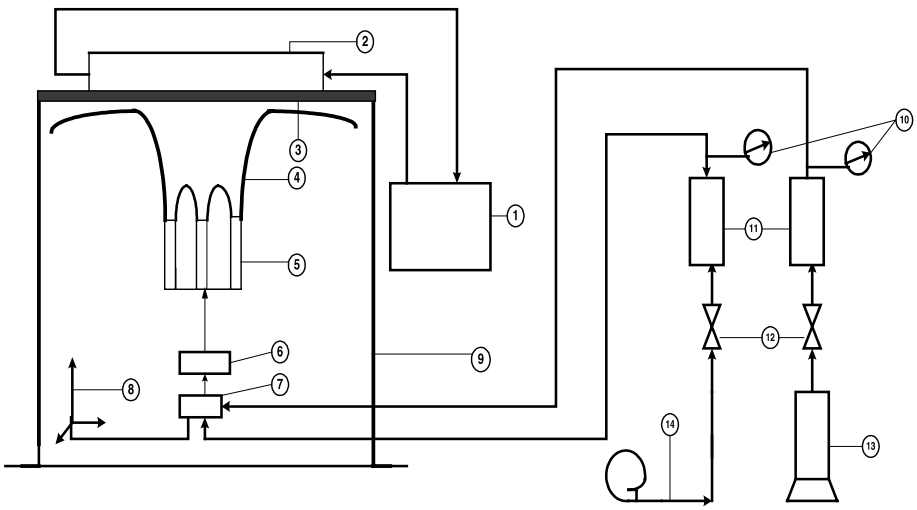

Fig. 1. Schematic of the experimental setup.

uniform exit velocity profile. The three-dimensional positioner enabled each of the attached burners to be fixed at a desired position related to the impingement surface.

The flame impingement surface was a rectangular copper plate of 200 mm long, 200 mm wide and 8 mm thick. It was evenly cooled on the backside by a cooling water jacket. Copper was selected because of its excellent thermal conductivity. The top plate of the cooling water jacket was made of plexiglass to visualize the water flow. A stainless steel frame was used to support the copper plate and the heat exchanger, such that the plate could be placed either horizontally or tilted at a selected angle related to the burner. After certain changes in the operating condition, measurements were only made after the steady-state condition had been established again and exit temperature of the cooling water had been stabilized. The cooling water temperatures were measured with K-type thermocouples.

The local heat flux from the flame to the plate was measured with a small ceramic heat flux transducer having an effective size of 3 mm × 3 mm × 0.08 mm, which was attached directly to the copper plate. Measurements of the heat flux distributions in the x- and y-directions were carried out by moving the burner positioner horizontally.

The surface temperatures of the impingement plate at the flame side were measured with 14 T-type thermocouples. Each thermocouple was embedded in a small hole, which was drilled from the rear of the copper plate to within 1 mm of the impingement side. Two lines of holes were drilled at distances away from the plate center, and they were perpendicular to each other, such that each thermocouple was spaced 15 mm apart from another. A PC-acquisitor was selected to record the heat fluxes and the plate temperatures simultaneously. The value of each heat flux and surface temperature presented here was the average of the data taken consecutively in 30 s at a rate of 500 samples/s.

3. Error analysis

The coordinate system used in the present study is shown in Fig. 2. An error analysis was performed with the method proposed by Kline and McClintock [42]. Using a 95% confidence level, the maximum and minimum uncertainties of the presented local heat flux were 13.3% and 3.4%, respectively. Combining the spatial uncertainty with the local heat flux uncertainty resulted in an uncertainty range of 4.3–14.2% for the area-averaged heat fluxes. Three tests with identical operating conditions were conducted and the results were found to be reproducible within these uncertainty ranges. The results of these three tests were then averaged.

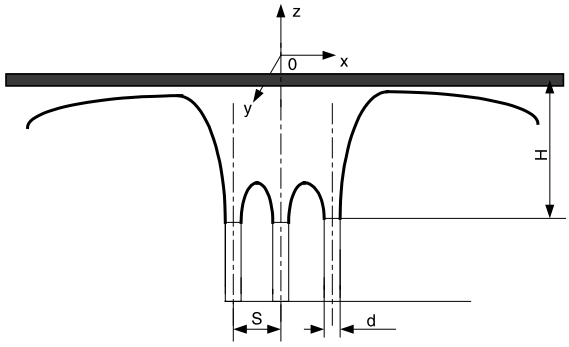

Fig. 2. Coordinate system of the impingement plate.

4. Results and discussion

Flame shapes and heat transfer results were obtained for laminar flames with a Reynolds number of 900 and an equivalence ratio of 1. Effects of the S/d and H/d ratios on flame shape and heat transfer rate of the impinging flame jets were examined.

4.1. The flame shape

Photographs of impinging flame jets with small, moderate and large jet-to-jet spacing (i.e., $S/d = 2.6$, 5, 7) under small H/d ratio of 2 and moderate H/d ratio of 5 are shown in Figs. 3–5. All the flames under consideration were found to be laminar. The flame from each single jet was observed to have a blue inner cone and a light blue outer layer. Due to interference between the jets, shapes of the center and the side jets were different. Moreover, the flame shapes were also affected by the S/d or H/d ratios.

It was found from Fig. 3(a) that for a small H/d ratio of 2, the inner cones impinged on the plate and then spread radially outwards. The deflected inner cone layers of the three jets almost connected to each other along the plate. The outer flame layers at the interacting side of the side jets did not impinge upwards, but merged with those of the center jet. There was a positive pressure at each of the interacting side, which forced the jets to move downwards and outwards. This resulted in the merge of the outer layers at the interacting sides exhibiting a "W-shape" for the whole flame. When the H/d ratio was increased to 5, it was found from Fig. 3(b) that the outer layers of the three jets coalesced with each other at the interacting side before impingement. The inner cones just reached the plate with no deflection observed. There was a slight outward shift of the tip of the inner cone of the side jets observed, which was due to the effect of the imbalance of the pressure between the interacting and non-interacting sides. It was observed from Fig. 3(c) and (d) that the wall jets spread in the

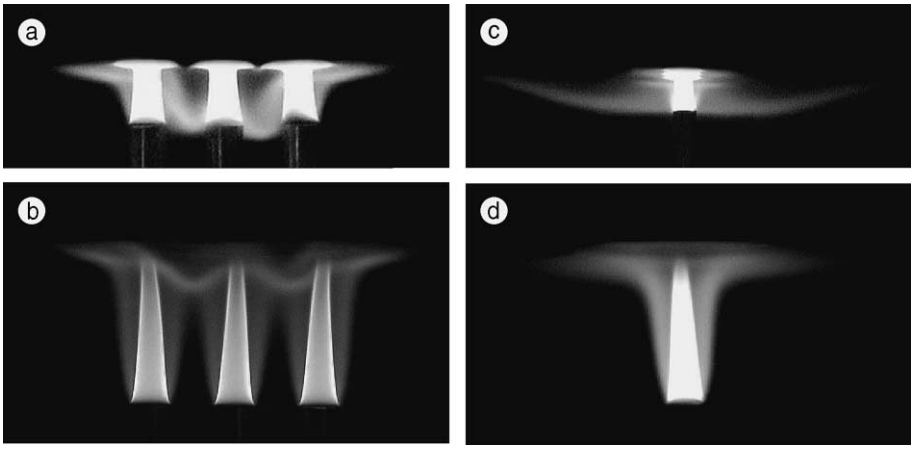

Fig. 3. Photographs of impinging flame jets viewed from x-direction (a) $Re = 900$; $S/d = 2.6$; $H/d = 2$; $\phi = 1$ and (b) $Re = 900$; $S/d = 2.6$; $H/d = 5$; $\phi = 1$. Photographs of impinging flame jets viewed from y-direction (c) $Re = 900$; $S/d = 2.6$; $H/d = 2$; $\phi = 1$ and (d) $Re = 900$; $S/d = 2.6$; $H/d = 5$; $\phi = 1$.

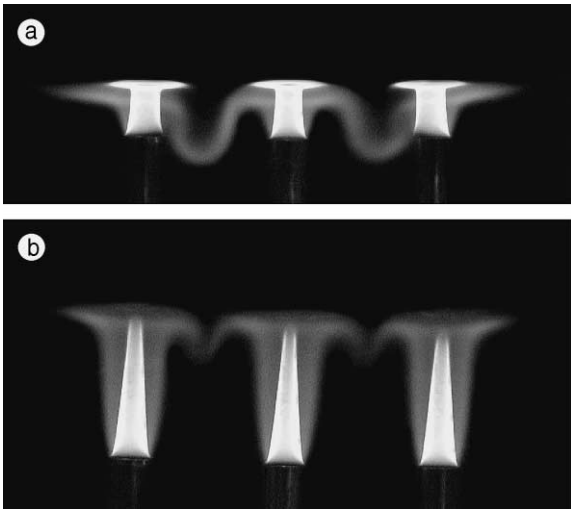

Fig. 4. Photographs of impinging flame jets viewed from x-direction (a) $Re = 900$; $S/d = 5$; $H/d = 2$; $\phi = 1$ and (b) $Re = 900$; $S/d = 5$; $H/d = 5$; $\phi = 1$.

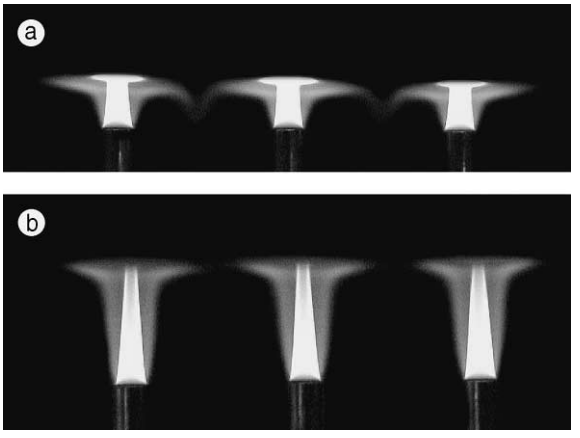

Fig. 5. Photographs of impinging flame jets viewed from x-direction (a) $Re = 900$; $S/d = 7$; $H/d = 2$; $\phi = 1$ and (b) $Re = 900$; $S/d = 7$; $H/d = 5$; $\phi = 1$.

y-direction after colliding with each other, which was also due to the pressure difference between the interacting zone and the ambient air. It could be observed that as the H/d ratio was increased from 2 to 5, this spent flow along the y-direction became less evident to indicate a weaker between-jet interference.

When the S/d ratio was increased to 5, it was observed from Fig. 4(a) and (b) that the between-jet interference became weaker, comparing to that obtained at the S/d ratio of 2.6 as shown in Fig. 3(a) and (b). It was evident that for $H/d = 2$, the wall jets of the center and side jets did not meet each other at the midpoint between them, but at a point shifted outwards. When the H/d ratio was increased to 5, this displacement of the meeting point from the midpoint of the neighboring jets became much smaller. This was due to the weaker between-jet interference. When the S/d ratio was further increased to 7, it was found from Fig. 5(a) that the between-jet interaction was only observed at the H/d ratio of 2. When the H/d ratio was increased to 5, this between-jet interference was not observed and all the three jets appeared to be a single jet respectively, as shown in Fig. 5(b).

4.2. Heat transfer

Effects of the S/d and H/d ratios on the local and area-averaged heat transfer rates from the impinging flame jets were examined in the present study.

4.2.1. Local heat transfer

4.2.1.1. Effect of the S/d ratio. The heat flux distributions under small and moderate H/d ratios of 2 and 5, with small, moderate and large S/d ratios of 2.6, 5 and 7, are shown in Figs. 6 and 7 respectively. The comparison of the heat flux distribution along the impingement line (i.e., the x-axis) at different S/d ratio with small and moderate H/d ratios of 2 and 5, are shown in Fig. 8.

It was found from Fig. 6(a) that for a small S/d ratio of 2.6 and a small H/d ratio of 2, the heat flux in the center jet area was relatively low. It was due to the impingement on the plate by the cold unreacted mixture in the central core of the center jet. It was further shown in Fig. 6(b) that there were altogether three locations of relatively low heat flux, i.e., the quasi-circular heat flux contour of the center jet and the quasi-elliptical contours of the two side jets. These three cool areas were almost connected with each other. For the side jets, it was found that the heat flux contour tend to be semi-circular as the radial distance from the jet center increased, which was due to the weaker between-jet interference at position far away from the central interacting zone. It was also observed that the center jet had lost the characteristics of

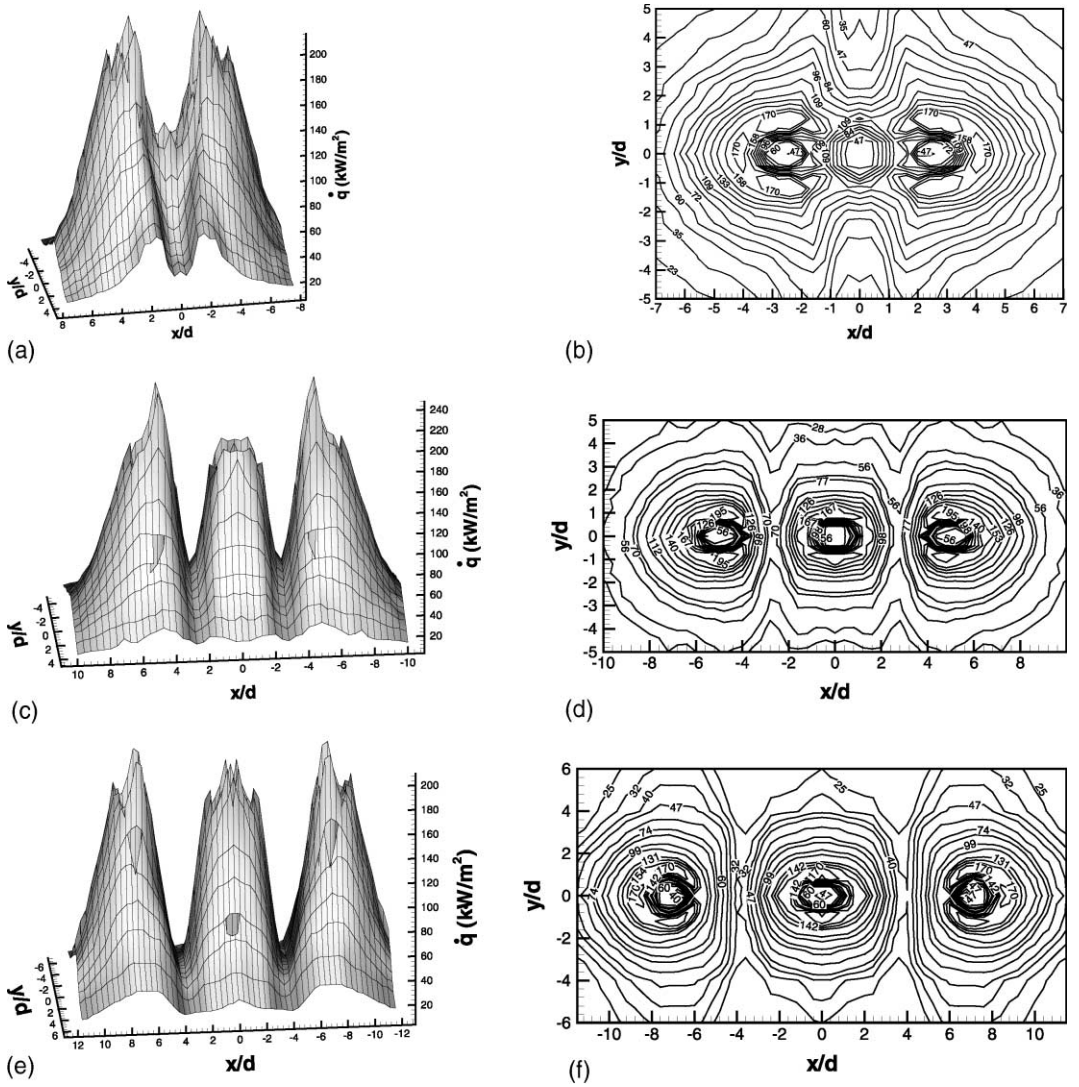

Fig. 6. (a) Three-dimensional heat flux distribution at $Re = 900$, $\phi = 1$, $H/d = 2$ and $S/d = 2.6$. (b) Heat flux contour at $Re = 900$, $\phi = 1$, $H/d = 2$ and $S/d = 2.6$. (c) Three-dimensional heat flux distribution at $Re = 900$, $\phi = 1$, $H/d = 2$ and $S/d = 5$. (d) Heat flux contour at $Re = 900$, $\phi = 1$, $H/d = 2$ and $S/d = 5$. (e) Three-dimensional heat flux distribution at $Re = 900$, $\phi = 1$, $H/d = 2$ and $S/d = 7$. (f) Heat flux contour at $Re = 900$, $\phi = 1$, $H/d = 2$ and $S/d = 7$.

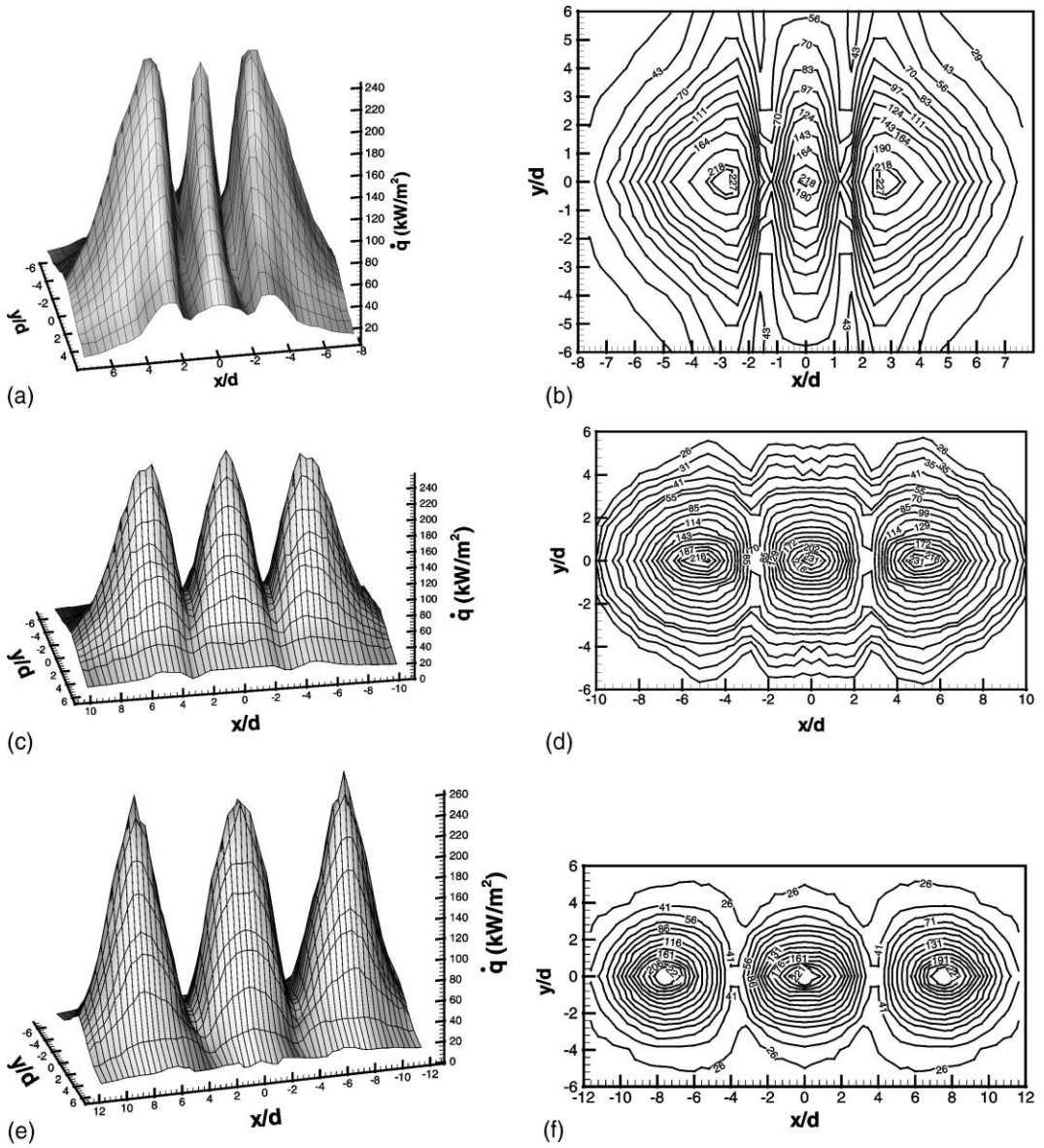

Fig. 7. (a) Three-dimensional heat flux distribution at $Re = 900$, $\phi = 1$, $H/d = 5$ and $S/d = 2.6$. (b) Heat flux contour at $Re = 900$, $\phi = 1$, $H/d = 5$ and $S/d = 2.6$. (c) Three-dimensional heat flux distribution at $Re = 900$, $\phi = 1$, $H/d = 5$ and $S/d = 5$. (d) Heat flux contour at $Re = 900$, $\phi = 1$, $H/d = 5$ and $S/d = 5$. (e) Three-dimensional heat flux distribution at $Re = 900$, $\phi = 1$, $H/d = 5$ and $S/d = 7$. (f) Heat flux contour at $Re = 900$, $\phi = 1$, $H/d = 5$ and $S/d = 7$.

a single jet, with no wall jet region formed because of the small jet-to-jet spacing.

When the S/d ratio was increased to 5, it was found from Fig. 6(c) that the heat flux distribution of the center jet was similar in shape to that of a single jet, which indicated that the between-jet interference was weaker when the S/d ratio was not at a moderate value of 5. The between-jet interference caused a higher heat flux gradient at the interacting sides than the non-interacting sides for all the three jets as shown in Fig. 6(d). This resulted in the quasi-rectangular heat flux contour for the center jet, and quasi-oval shapes for the side jets. It could also be found from Fig. 6(d) that the heat flux contours of the center and the side jets did not meet each other at the midpoint (i.e., $X/d = 2.5$) of the two adjacent jets, but at a point of when $X/d = 2.8$. This phenomenon was in agreement with that had been found in the flame structure as shown in Fig. 4(a). As stated

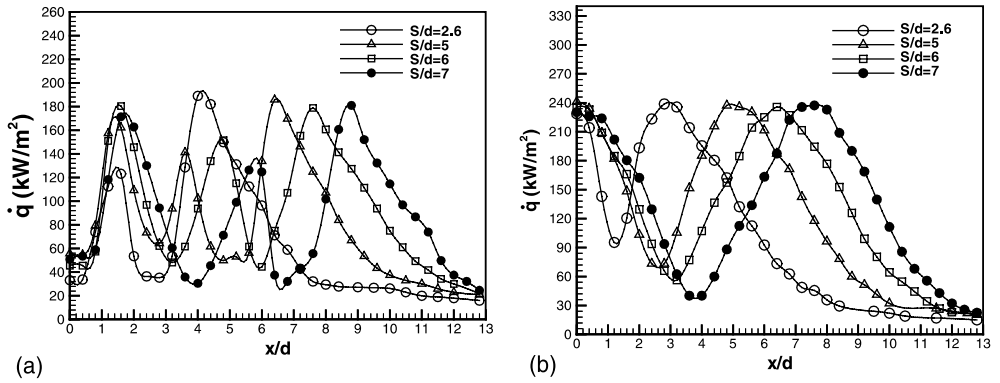

Fig. 8. Effect of S/d on heat flux distribution from flame to the plate at x-axis at (a) $Re = 900$, $\phi = 1$, $H/d = 2$ and (b) $Re = 900$, $\phi = 1$, $H/d = 5$.

before, the compressed heat flux contours at the interacting sides were caused by the pressure difference.

When the S/d ratio was further increased to 7 from 5, the between-jet interference was further reduced, as shown in Fig. 6(e) and (f). Only a slight compression of the heat flux contours was found at the interacting side for all the center and side jets. The center jet exhibited more characteristics of a single jet.

The heat flux distributions for the jets under a moderate H/d ratio of 5 are shown in Fig. 7. It was found that when the H/d ratio was increased to 5, the cool central areas with low heat fluxes of the center and side jets disappeared. On the contrary, the maximum heat flux occurred in this central area for $S/d = 2.6$, 5 and 7. It was found from Fig. 7(b) that very large heat flux gradients existed between the two adjacent jets, which led to more non-uniform heating in these areas. When the S/d ratio was increased to 5 from 2.6, the heat flux contour of the center jet was less compressed in the x-direction. When the S/d ratio was further increased to 7, it was found from Fig. 7(f) that all the jets behaved almost like a separate single jet.

Because of the symmetrical geometry at both sides of the centerline of the center jet, only the heat flux distribution on the right-hand side has been presented in Figs. 8, 9 and 11. Comparison of heat flux distributions along the x-axis for different S/d ratio at a H/d ratio of 2 and 5 are shown in Fig. 8. It was found from Fig. 8(a) that with $H/d = 2$, the distribution curves for $S/d \geqslant 5$ were similar, with three peaks and three troughs existed. The first peak occurred in the center jet and the other two in the side jet. One trough occurred at the point where the two spreading wall jets were meeting each other, whereas the other two troughs occurred at the centers of the center jet and the side jet. When $S/d = 2.6$, only two peaks and two minimum points were found because the deflected inner cone layers of the center jet and the side jet met each other at a location very close to the plate. An overlap of the peaks of the center jet and the side jet occurred at the point where the spreading wall jets were meeting each other at the interacting side. This peak occurred at about $S/d = 1.6$ with a slight outwards shift from the between-jet midpoint. It was also found that the peak heat flux of the center jet and that of the side jet at the non-interacting side were nearly equal to each other, but the peak heat flux of the side jet at the interacting side was lower. It was due to the positive pressure at the interacting zone caused by the uneven flow of fuel/air mixture of the side jet in the inward and outward directions with more mixture flowing outwards. It was also found that location of the between-jet minimum heat flux was not at the between-jet midpoint, but at some distance shifted outwards as found in the flame photographs and the heat flux contours.

When the H/d ratio was increased to 5, it was found from Fig. 8(b) that all the four curves were of the similar trend. Each of them had two peaks and one trough. All the peak values occurred near the centers of the jets, because the tips of the flame inner cones just reached the plate as shown in Figs. 3(b), 4(b) and 5(b). The high temperatures in this reaction zone enhanced the heat transfer rate, resulting in the maximum heat flux at the place where the inner cone tip of the flame contacted the impingement plate. The minimum heat flux occurred at the point where the spreading wall jets of the center and the side jets were meeting each other, just as the case for $H/d = 2$. This minimum heat flux increased with reducing S/d. It was also found from Fig. 8(b) that for $S/d \leqslant 6$, asymmetric heat flux distribution occurred on the two sides of the side jet. The heat flux decreased more quickly at the interacting side than the non-interacting side, and this asymmetry became trivial when the S/d ratio was increased to 7, which was also indicated in the heat flux contours.

4.2.1.2. Effect of the H/d ratio. The comparison of the heat flux distributions along the impingement line (i.e.,

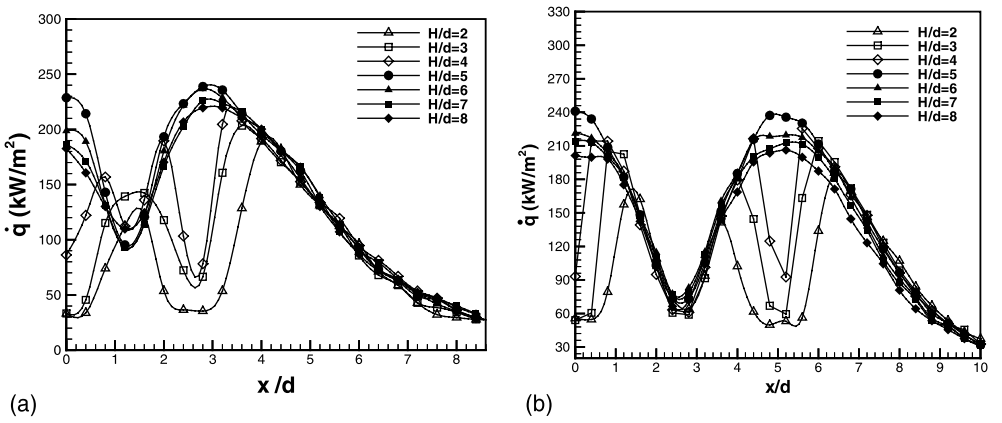

Fig. 9. Effect of H/d on heat flux distribution from flame to the plate at x-axis at (a) $Re = 900$, $\phi = 1$, $S/d = 2.6$ and (b) $Re = 900$, $\phi = 1$, $S/d = 5$.

x-axis) under different H/d ratio with small and moderate S/d ratios of 2.6 and 5 are shown in Fig. 9. It was found from Fig. 9(a) that with small S/d ratio of 2.6, for all the H/d ratios from 2 to 8, distinct difference between the heat fluxes were only found at $x/d \leqslant 4$. This indicated that the H/d ratio had almost no influence on heat transfer in the late wall jet region of $x/d > 4$. Three kinds of distribution trend were found. The first one was for the curves obtained at $H/d \leqslant 3$, with the occurrence of two peaks and two troughs. The two troughs occurred at the center of the center and the side jets. The first peak was due to the merge of the peaks of the center and the side jets at the interacting zone. Lower heat flux was associated with lower H/d because of the suppression of combustion. When the H/d ratio was increased to 4, three peaks and three minimum points were found. Due to weaker between-jet interference, the two peaks which had been merged at lower H/d ratio were separating into distinct peaks and at the same time generating a minimum heat flux between them. When $H/d \geqslant 5$, the distribution curves were similar with two peaks at the jet centers and one minimum heat flux at the jets' meeting point. When the H/d ratio was larger than 5, a gradual reduction of heat flux was found.

The comparison of the effect of H/d ratio on heat transfer with moderate S/d ratio of 5 is shown in Fig. 9(b). It was found that the heat flux difference between different H/d ratios was obscure when $x/d \geqslant 7$. Minimum heat fluxes with similar values occurred at the points where the two wall jets were meeting each other (i.e., $x/d = 2.5$), for all the flames with the H/d ratios ranged from 2 to 8. Two types of distribution trend were observed. The first one was occurred when $H/d \leqslant 4$, where three peaks and three minimum points were found, which had been discussed before for the case at $H/d = 2$. The influence of the cool central core became weaker when the H/d ratio was increased, which was indicated by the gradual increase of the first and the third minimum points, and the outward shifting of the first peak and the inward shifting of the second peak. When the H/d ratio reached 5, the maximum heat flux was obtained at both the stagnation points of the center and the side jets. The heat flux began to decrease gradually when the H/d ratio was further increased, as the case at $S/d = 2.6$. This reduction was only evident in both the impingement regions of the center and the side jets, as shown in Fig. 9(b).

4.2.2. Average heat flux

The average heat flux deserves more concern in many practical applications. The surface-averaged heat fluxes were obtained by integrating the local values of the center jet, the side jets and the total jet array, respectively. The main purpose is to compare the heating capabilities of both the center and the side jets under different S/d and H/d ratios. The integrating areas were both square with a side length of S as shown in Fig. 10(a), which was the same to that selected by Huber [2] in his study of multiple impinging air jets. The area-averaged heat flux was obtained by

$$\bar{q} = \frac{1}{A}\int\int_A \dot{q}\,\mathrm{d}A = \frac{\int_0^S \int_0^S \dot{q}(x,y)\,\mathrm{d}x\,\mathrm{d}y}{S^2} \tag{1}$$

The area-averaged heat fluxes of the center jet, the side jets and the total jet array, with different S/d ratios of 2.6, 5 and 7, and different H/d ratios of 2 and 5, are shown in Fig. 10(b).

It was found that at a certain S/d ratio, the average heat flux at the H/d ratio of 2 was lower than that at the moderate H/d ratio of 5. It was because the cool central core with low heat flux occurred at $H/d = 2$, and disappeared when the H/d ratio was increased to 5. It was found that at $H/d = 2$ and $S/d = 2.6$, a large difference

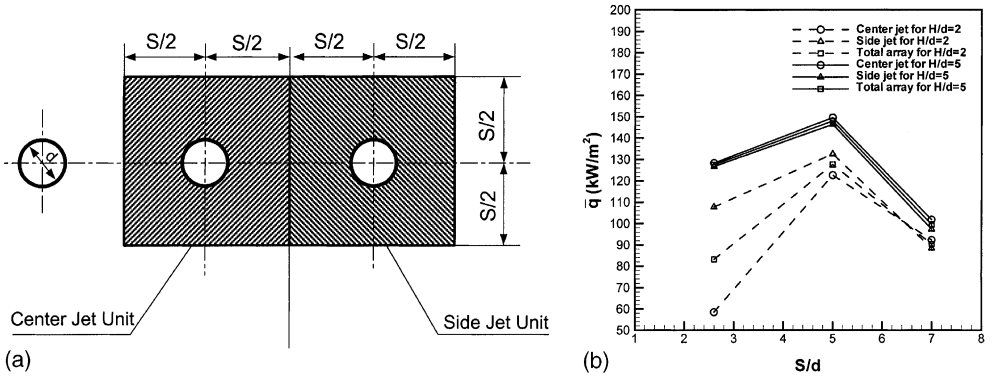

Fig. 10. (a) Integration area for the center and the side jets. (b) Comparisons of area-averaged heat flux of the center and the side jets at $Re = 900$ and $\phi = 1$.

in average heat flux between the center jet, the side jets and the total jet array was obtained. The average heat flux of the side jet unit was the largest and that of the center jet unit was the lowest. This is because the between-jet interference induced heat transfer suppression is much accentuated when both the H/d and S/d ratios are low. The center jet suffered from this interference at both two sides, but it was only one side for the side jet, thus the average heat flux of the center jet unit was lower. When the S/d ratio was increased to 5, the same trend was still observed except that the difference became much smaller. This is because at the moderate S/d ratio of 5, the between-jet interference is weak, which led to a weak overall interference compared to that at the S/d ratio of 2.6, and therefore the average heat flux difference became smaller. When the S/d ratio was further increased to 7, there was almost no difference between the average heat flux as the difference was within the uncertainty range. It indicated that the heating capabilities of the center jet and the side jets were almost the same when the S/d ratio was large enough. This is because a very weak between-jet interference is experienced at the large S/d ratio of 7. It was observed that when the H/d ratio was at a moderate value of 5, rather trivial average heat flux difference was found for all the S/d ratios being considered. Furthermore, these differences were within the uncertainty range. This indicated that at a small H/d ratio of 2, heating capacities of the center and the side jets were different at small and moderate S/d ratios. However, when the H/d ratio was at a moderate value of 5, heating capacities of the center and the side jets were similar at the S/d ratios being investigated.

It was also found that for both H/d ratios of 2 and 5, the maximum average heat flux occurred at $S/d = 5$. Further increase or decrease of the S/d ratio reduced the average heat flux. This variation trend was in agreement with the characteristics of multiple impinging air jets obtained by Obot and Trabold [16] and Huber [2].

4.2.3. Comparison with single jet

To examine the difference in heat transfer characteristics between a single flame jet and the in-line three-jets system, experiments were performed with a single flame jet under similar conditions. The two typical H/d ratios of 2 and 5 were selected. The local heat flux distribution along the x-axis of a single jet was compared to that of the multiple jets with a S/d ratio of 7, as shown in Fig. 11. It was found from Fig. 11(a) that at $H/d = 2$ both stagnation point and maximum heat fluxes were enhanced with the multiple jets, with the maximum heat flux increased almost by 50%. The maximum heat flux also increased by more than 50% at $H/d = 5$, as shown in Fig. 11(b). This heat transfer augmentation was due to the enhanced turbulence in the between-jet area. Carcasci [43] found that two types of vortex were occurring in the between-jet area, which increased the turbulence significantly, and thus the combustion and heat transfer.

Comparison of the stagnation point heat flux of the center jet with those of a single jet obtained experimentally and semi-analytically is shown in Fig. 12. The semi-analytical solution of the stagnation point heat flux of a single circular flame jet was obtained from the following equation, according to Tariq [44]:

$$\dot{q} = 0.763\beta^{0.5}(\overline{\rho\mu})^{0.5}(\overline{Pr}_f)^{-0.6} \times \{1 + (\overline{Le}_H - 1)\Delta h_{chem,H}/\Delta h_{eq}\}^{0.6}\Delta h_{eq} \quad (2)$$

Assuming Lewis number to be unity, Eq. (2) can be rewritten as:

$$\dot{q} = 0.763\beta^{0.5}(\overline{\rho\mu})^{0.5}(\overline{Pr}_f)^{-0.6}\Delta h_{eq} = 0.763\beta^{0.5}(\overline{\rho\mu})^{0.5}(\overline{Pr}_f)^{-0.6}C_{P_{eq}}(T_e - T_w) \quad (3)$$

Based on the potential flow solution for flow normal to a disk [45]:

$$\beta = 4u/\pi D_b \quad (4)$$

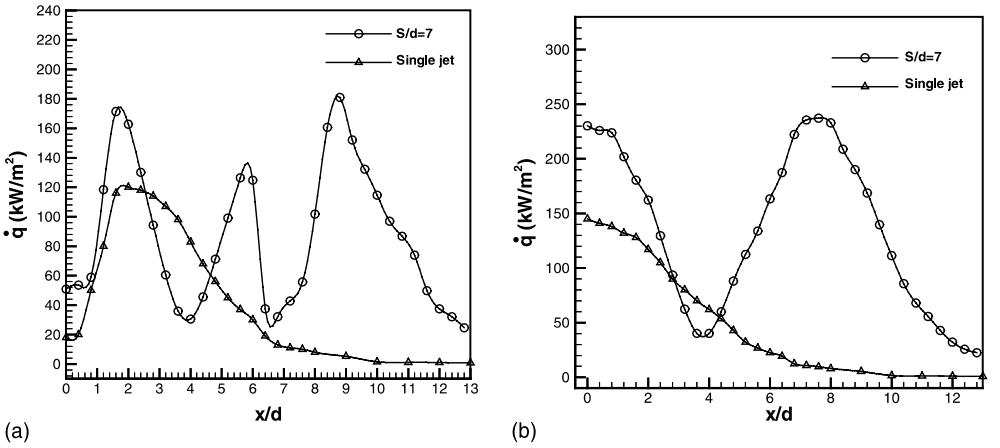

Fig. 11. Comparison of local heat flux distribution with single jet at (a) $Re = 900$, $\phi = 1$, $H/d = 2$ and (b) $Re = 900$, $\phi = 1$, $H/d = 5$.

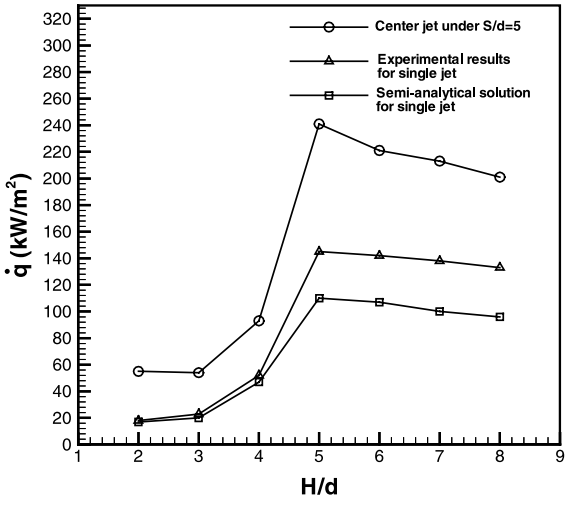

Fig. 12. Comparison of stagnation point heat flux with single jet at $Re = 900$ and $\phi = 1$.

It was observed from Fig. 12 that the stagnation point heat flux of the center jet in the three-jet array was always greater than that of a single jet for the H/d ratios ranged from 2 to 8. The heat flux difference between the experimental result and the semi-analytical solution was small when $H/d \leqslant 4$, but such difference became larger when $H/d \geqslant 5$. This is because the Lewis number augmentation has been ignored in the semi-analytical solution. When $H/d \leqslant 4$, the flame temperature was lower at the stagnation point because of the direct impingement of the cold unreacted gas and the Lewis number augmentation effect was not significant. However, the flame temperature at the stagnation point increased greatly at $H/d \geqslant 5$ due to the occurrence of the reaction zone around this point. The augmented heat transfer in the dissociation–recombination process was evident, and the Lewis number was deviated from unity. The Lewis number was maintained unity in the semi-analytical solution, which resulted in the bigger difference between the experimental result and the semi-analytical prediction.

5. Conclusions

1. A positive pressure will be formed at the between-jet interacting zone when two adjacent jets meet and collide with each other. This pressure causes the flow in the interacting zone to move downwards and outwards, where a relatively low atmospheric pressure existed. As a result, the spreading wall jets of the center and the side jets do not meet each other at the between-jet midpoint, but at a location some distance shifted outwards. Moreover, the local heat transfer distributions on the two sides of a side jet are asymmetric.
2. The between-jet interference reduces the heat transfer in the interacting zone. This heat transfer depression effect becomes stronger when the S/d and H/d ratios are small. More fuel/air mixture are flowing outwards from the side jet, resulting in a lower maximum heat transfer at the interacting side and a faster reduction of the local heat transfer rate than that at the non-interacting side.
3. Small H/d and S/d ratios also reduce the area-averaged heat flux. This depression becomes more evident when both the H/d and S/d ratios are small. The highest heat transfer is obtained when both the H/d and S/d ratios are at a moderate value of 5, at which both the local and maximum heat fluxes are reaching

their maximum values. The lowest area-averaged heat flux is obtained when $H/d = 2$ and $S/d = 2.6$.

4. In a row of three-jet systems, the stagnation and the maximum heat fluxes of both the center and the side jets are greater than those of a single jet operating with the same experimental conditions, which indicates an enhanced heat transfer capabilities of a flame jet in an jet array.

Acknowledgements

The authors wish to thank the Hong Kong Polytechnic University for financial support of the present study (project code: GV-323).

References

[1] B.R. Hollworth, R.D. Berry, Heat transfer from arrays of impinging jets with large jet-to-jet spacing, J. Heat Transfer 100 (1978) 352–357.
[2] A.M. Huber, Heat transfer with impinging gaseous jet systems, Ph.D. thesis, Purdue University, 1993.
[3] J.M.M. Barata, D.F.G. Durao, M.V. Heitor, Impingement of single and twin turbulent jets through a crossflow, AIAA J. 29 (1991) 595–602.
[4] J.M.M. Barata, D.F.G. Durao, M.V. Heitor, Velocity characteristics of multiple impinging jets through a crossflow, J. Fluids Eng. 114 (1992) 231–239.
[5] R.J. Kind, K. Suthanthiran, The interaction of two opposing plane turbulent wall jets, in: AIAA paper 72-211: AIAA 10th Aerospace Sciences meeting, San Diego, CA, 1972.
[6] E. Tanaka, The interference of two-dimensional parallel jets (first report, experiments on dual jet), Bull. JSME 13 (1970) 272–280.
[7] E. Tanaka, The interference of two-dimensional parallel jets (second reports, experiments on the combined flow of dual jet), Bull. JSME 17 (1974) 920–927.
[8] X. Yan, N. Saniei, Measurements of local heat transfer coefficients from a flat plate to a pair of circular air impinging jets, Exp. Heat Transfer 9 (1996) 29–47.
[9] S. Mikhail, S.M. Morcos, M.M.M. Abou-Ellail, W.S. Ghaly, Numerical prediction of flow field and heat transfer from a row of laminar slot jets impinging on a flat plate, Heat Transfer (3) (1982) 377–382.
[10] S.J. Slayzak, R. Viskanta, F.P. Incropera, Effects of interactions between adjoining rows of circular, free-surface jets on local heat transfer from the impingement surface, J. Heat Transfer 116 (1994) 88–95.
[11] L.W. Florschuetz, C.C. Su, Effects of crossflow temperature on heat transfer within an array of impinging jets, J. Heat Transfer 109 (1987) 74–82.
[12] L.W. Florschuetz, C.R. Truman, D.E. Metzger, Streamwise flow and heat transfer distributions for jet array impingement with crossflow, J. Heat Transfer 103 (1981) 337–342.
[13] R. Gardon, J.C. Akfirat, Heat transfer characteristics of impinging two-dimensional air jets, J. Heat Transfer 88 (1966) 101–108.
[14] A.I. Behbahani, R.J. Goldstein, Local heat transfer to staggered arrays of impinging circular air jets, J. Eng. Power 105 (1983) 354–360.
[15] A.M. Huber, R. Viskanta, Comparison of convective heat transfer to perimeter and center jets in a confined, impinging array of axisymmetric air jets, Int. J. Heat Mass Transfer 37 (1994) 3025–3030.
[16] N.T. Obot, T.A. Trabold, Impingement heat transfer within arrays of circular jets. Part 1: effects of minimum, intermediate, and complete crossflow for small and large spacings, J. Heat Transfer 109 (1987) 872–879.
[17] K.W. Van Treuren, Z. Wang, P.T. Ireland, T.V. Jones, Detailed measurements of local heat transfer coefficient and adiabatic wall temperature beneath an array of impinging jets, J. Turbomach. 116 (1994) 369–374.
[18] A.H. Shiravi, A.S. Mujumdar, G.J. Kubes, Numerical study of heat transfer and fluid flow in multiple turbulent impinging jets, Drying Technol. 13 (1995) 1359–1375.
[19] P. Hrycak, Heat transfer from a row of impinging jets to concave cylindrical surfaces, Int. J. Heat Mass Transfer 24 (1981) 407–419.
[20] H. Laschefski, T. Cziesla, G. Biswas, N.K. Mitra, Numerical investigation of heat transfer by rows of rectangular impinging jets, Numer. Heat Transfer—Part A 30 (1996) 87–101.
[21] S.H. Seyedein, M. Hasan, A.S. Mujumdar, Turbulent flow and heat transfer from confined multiple impinging slot jets, Numer. Heat Transfer—Part A 27 (1995) 35–51.
[22] N.R. Saad, S. Polat, W.J.M. Douglas, Confined multiple impinging slot jets without crossflow effects, Int. J. Heat Fluid Flow 13 (1992) 2–14.
[23] R.J. Goldstein, J.F. Timmers, Visualization of heat transfer from arrays of impinging jets, Int. J. Heat Mass Transfer 25 (1982) 1857–1868.
[24] R.J. Goldstein, W.S. Seol, Heat transfer to a row of impinging circular air jets including the effect of entrainment, Int. J. Heat Mass Transfer 34 (1991) 2133–2147.
[25] R.N. Koopman, E.M. Sparrow, Local and average transfer coefficients due to an impinging row of jets, Int. J. Heat Mass Transfer 19 (1976) 673–683.
[26] K. Ichimiya, Numerical estimation on impingement heat transfer caused by confined three slot jets, in: J.A. Reizes (Ed.), Transport Phenomena in Heat and Mass Transfer, 1992, pp. 456–457.
[27] M. Gundappa, J.F. Hudson, T.E. Diller, Jet impingement heat transfer from jet tubes and orifices, in: National Heat Transfer Conference HTD-107, 1989, pp. 43–50.
[28] S. Al-Sanea, A numerical study of the flow and heat transfer characteristics of an impinging laminar slot-jet including crossflow effects, Int. J. Heat Mass Transfer 35 (1992) 2501–2513.
[29] S.H. Seyedein, M. Hasan, A.S. Mujumdar, Laminar flow and heat transfer from multiple impinging slot jets with an inclined confinement surface, Int. J. Heat Mass Transfer 37 (1994) 1867–1875.
[30] C.E. Baukal, B. Gebhart, Surface condition effects on flame impingement heat transfer, Exp. Thermal Fluid Sci. 15 (1997) 323–335.

[31] L.L. Dong, C.S. Cheung, C.W. Leung, Heat transfer from an impinging premixed butane/air slot flame jet, Int. J. Heat Mass Transfer 45 (2002) 979–992.
[32] M. Fairweather, J.K. Kilham, S. Nawaz, Stagnation point heat transfer from laminar, high temperature methane flames, Int. J. Heat Fluid Flow 5 (1) (1984) 21–27.
[33] G.K. Hargrave, J.K. Kilham, The effect of turbulence intensity on convective heat transfer from premixed methane-air flames, Inst. Chem. Eng. Symp. Ser. 2 (1984) 1025–1034.
[34] K. Kataoka, H. Shundoh, H. Matsuo, Convective heat transfer between a flat plate and a jet of hot gas impinging on it, Drying '84 (1984) 218–227.
[35] J.R. Rigby, B.W. Webb, An experimental investigation of diffusion flame jet impingement heat transfer, in: Proceedings of the ASME/JSME Thermal Engineering Joint Conference, vol. 3, 1995, pp. 117–126.
[36] Th.H. Van der Meer, Stagnation point heat transfer from turbulent low Reynolds number jets and flame jets, Exp. Thermal Fluid Sci. 4 (1991) 115–126.
[37] G.K. Malikov, D.L. Lobanov, Y.K. Malikov, V.G. Lisienko, R. Viskanta, A.G. Fedorov, Experimental and numerical study of heat transfer in a flame jet impingement system, J. Inst. Energy 72 (1999) 2–9.
[38] J.W. Mohr, J. Seyed-Yagoobi, R.H. Page, Heat transfer from a pair of radial jet reattachment flames, J. Heat Transfer 119 (1997) 633–635.
[39] J. Wu, J. Seyed-Yagoobi, R.H. Page, Heat transfer and combustion characteristics of an array of radial jet reattachment flames, Combust. Flame 125 (2001) 955–964.
[40] R. Viskanta, Heat transfer to impinging isothermal gas and flame jets, Exp. Thermal Fluid Sci. 6 (1993) 111–134.
[41] R. Viskanta, Convective and radiative flame jet impingement heat transfer, in: The Ninth International Symposium on Transport Phenomena in Thermal-Fluids Engineering, 1996, pp. 46–60.
[42] S.J. Kline, F.A. McClintock, Describing uncertainties in single-sample experiments, Mech. Eng. 75 (1953) 3–8.
[43] C. Carcasci, An experimental investigation on air impinging jets using visualization methods, Int. J. Thermal Sci. 38 (1999) 808–818.
[44] A.S. Tariq, Impingement heat transfer from turbulent and laminar flames, Ph.D. thesis, Portsmouth Polytechnic, 1982.
[45] Th.H. Van der Meer, Heat transfer from impinging flame jets, Ph.D. thesis, Delft University of Technology, Netherlands, 1987.